Star-Shaped and Linear Terthiophene-thiol Self-assembled Monolayers as Scaffolds for Gold Nanoparticles

B. Vercelli and G. Zotti*

Istituto per l'Energetica e le Interfasi, Consiglio Nazionale delle Ricerche, c.o Stati Uniti 4, 35127 Padova, Italy

A. Berlin*

Istituto di Scienze e Tecnologie Molecolari, Consiglio Nazionale delle Ricerche, via C.Golgi 19, 20133 Milano, Italy

Received October 3, 2006. Revised Manuscript Received November 22, 2006

Self-assembled monolayers (SAMs) on gold of a new terthiophene-armed star-shaped molecule are reported. Oxidative coupling of the terthiophene (T3) ends leads to sexithiophene (T6) surface bridges. Surface plasmon spectroscopy has evidenced the ability of the T3- and T6-monolayers to coordinate gold nanoparticles. The kinetics of gold nanoparticle monolayer formation on T3- and thiol-primed surfaces has been investigated. Multilayers of oligothiophene-thiol and gold nanoparticles have been produced and compared with the analogous structures from a linear terthiophene-thiol and a generic star-shaped tetrathiol. SAMs and multilayers were characterized by CV, UV−vis, conductivity, and AFM. The conductivity of the oligothiophene-based gold multilayers is comparable with that (0.05 S cm^{-1}) of the tetrathiol-gold multilayer.

1. Introduction

The use of polyconjugated oligomers or polymers in self-assembled monolayers (SAMs)[1] is promising for optoelectronic applications and for molecular electronics.[2,3] In fact, SAMs may be initiator systems for the preparation of uniform and densely grafted polymer brushes[4−7] and in particular linear oligothiophenes have shown such ability.[8]

After it was reported that terthiophene (T3) may be adsorbed on gold surfaces,[9] we have been investigating the ability of T3-based monolayers to coordinate gold nanoparticles to produce novel materials containing this technologically new form of gold.[10] The use of conjugated chains to link gold nanoparticles is of particular interest for the modulation of conduction, charge transfer, and optical properties of materials based on gold nanoparticles.

Advincula and co-workers recently reported the synthesis of dendrimers functionalized with terthiophene dendrons on their periphery and dendrimer-encapsulated gold nanoparticles,[11] though no clear evidence of definite composition was given.

In this study we have considered both a molecule with a single terthiophene end as the gold-interactive moiety and a molecule in which the activity of the moiety is enhanced via the presence in multiple arms, which may be performed with dendrimers. Reported thiophene-based dendrimers, if not fully thiophene-based,[12] bear thiophene or oligothiophene moieties as the molecular core[13] or at the dendrimer surface.[14] More specific are star-shaped molecules in which the oligothiophene arms are generated from a triphenylamine[15] or from a benzene core.[16] In the latter case oxidation leads to coupling at the free α-positions with formation of a polymer network. In all cases the arms of the

* To whom correspondence should be addressed. G. Zotti: tel., (+39)49-8295868; fax, (+39)49-8295853; e-mail, g.zotti@ieni.cnr.it.

(1) (a) Kumar, A.; Abbott, N. L.; Kim, E.; Biebuick, H. A.; Whitesides, G. M. *Acc. Chem. Res.* **1995**, *28*, 219. (b) Ulman, A. *Chem. Rev.* **1996**, *96*, 1533.
(2) Fabre, B.; Wayner, D. D. M. *Langmuir* **2003**, *19*, 7145.
(3) Liang, Z.; Rackaitis, M.; Li, K.; Manias, E.; Wang, Q. *Chem. Mater.* **2003**, *15*, 2699.
(4) Shah, R. R.; Merreceyes, D.; Husemann, M.; Rees, I.; Abbott, N. L.; Hawker, C. J.; Hedrick, J. L. *Macromolecules* **2000**, *33*, 597.
(5) Zhou, F.; Liu, W.; Hao, J.; Xu, T.; Chen, M.; Xue, Q. *Adv. Funct. Mater.* **2003**, *13*, 938.
(6) Schmelmer, U.; Jordan, R.; Geyer, W.; Eck, W.; Golzhauser, A.; Grunze, M.; Ulman, A. *Angew. Chem., Int. Ed.* **2003**, *42*, 559.
(7) (a) Biesalski, M.; Ruhe, J. *Macromolecules* **2004**, *37*, 2196. (b) Ma, H.; Hyun, J.; Stiller, P.; Chilkoti, A. *Adv. Mater.* **2004**, *16*, 338.
(8) Zotti, G.; Zecchin, S.; Vercelli, B.; Berlin, A.; Grimoldi, S.; Groenendaal, L.; Bertoncello, R.; Natali, M. *Chem. Mater.* **2005**, *17*, 3681.
(9) (a) Matsumura, T.; Shimoyama, Y. *Eur. Phys. J.* **2002**, *7*, 233. (b) Mishina, E.; Miyakita, Y.; Yu, Q. K.; Nakabayashi, S.; Sakaguchi, H. *J. Chem. Phys.* **2002**, *117*, 4016.
(10) Daniel, M. C.; Astruc, D. *Chem. Rev.* **2004**, *104*, 293.
(11) Deng, S.; Locklin, J.; Patton, D.; Baba, A.; Advincula, R. C. *J. Am. Chem. Soc.* **2005**, *127*, 1744.
(12) (a) Xia, C.; Fan, X.; Locklin, J.; Advincula, R. C. *Org. Lett.* **2002**, *4*, 2067. (b) Xia, C.; Fan, X.; Locklin, J.; Advincula, R. C.; Gies, A.; Nonidez, W. *J. Am. Chem. Soc.* **2004**, *126*, 8735. (c) Nakayama, J.; Lin, J. S. *Tetrahedron Lett.* **1997**, *38*, 6043.
(13) (a) Jestin, I.; Levillain, E.; Roncali, J. *Chem. Commun.* **1998**, *23*, 2655. (b) Adronov, A.; Malenfant, P. R. L.; Frechet, J. M. J. *Chem. Mater.* **2000**, *12*, 1463. (c) Malenfant, P. R. L.; Groenendaal, L.; Frechet, J. M. J. *J. Am. Chem. Soc.* **1998**, *120*, 10990. (d) Malenfant, P. R. L.; Frechet, J. M. J. *Macromolecules* **2000**, *33*, 3634. (e) Apperloo, J. J.; Janssen, R. A. J.; Malenfant, P. R. L.; Groenendaal, L.; Fréchet, J. M. J. *J. Am. Chem. Soc.* **2000**, *122*, 7042. (f) Furuta, P.; Fréchet, J. M. J. *J. Am. Chem. Soc.* **2003**, *125*, 13173. (g) Otsubo, T.; Ueno, S.; Takimiya, K.; Aso, Y. *Chem. Lett.* **2004**, *33*, 1154. (h) Vestberg, R.; Nilsson, C.; Lopes, C.; Lind, P.; Eliasson, B.; Malmstroem, E. *J. Polym. Sci., Part A* **2005**, *43*, 1177.

10.1021/cm062362x CCC: $37.00
Published on Web 01/12/2007

Chart 1

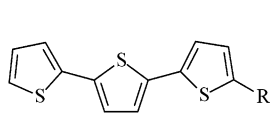

R = -$(CH_2)_6$SH **T3C6SH**
-SH **T3SH**
-$(CH_2)_6PO_2H_3$ **T3C6PA**

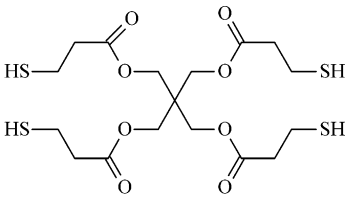

MP4

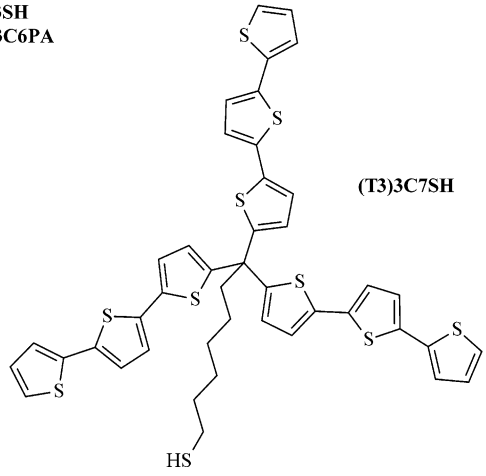

(T3)3C7SH

oligothiophene star are coplanar with the plane of the benzene ring.

A benzene ring does not allow surface linking with the star ends disposed in a plane parallel to the surface, but a four-arm carbon atom would allow three arms to extend over such a plane and thereby interact mutually. For this reason we have synthesized the star molecule (T3)3C7SH (Chart 1) with three terthiophene arms and a hexylthiol linker stemming from the same carbon atom. In this structure the distance between the end points of the terthiophene arms is ca. 2.1 nm.

We have then investigated the formation of SAMs on gold electrodes of such oligothiophene-armed star-shaped molecule, the surface coupling processes of the monolayers to sexithiophene (T6) surface bridges, and the ability of the monolayers to coordinate gold nanoparticles (5 nm diameter). Multilayers of this oligothiophene-thiol and gold nanoparticles have also been produced and compared with the analogous structures obtained from the linear terthiophene-thiol T3C6SH and the star-shaped nonconjugated tetrathiol MP4 (Chart 1). SAMs and multilayers were characterized by CV, UV−vis, conductivity, and AFM.

2. Experimental Section

2.1. Chemicals and Reagents. All melting points are uncorrected. All reactions of air- and water-sensitive materials were performed under nitrogen. Air- and water-sensitive solutions were transferred with double-ended needles. The solvents used in the reactions (Fluka) were absolute and stored over molecular sieves. Acetonitrile was reagent grade (Uvasol, Merck) with a water content <0.01%. The star-shaped tetrathiol pentaerythritol tetrakis(3-mercaptopropionate) (MP4) was from Aldrich. The supporting electrolyte tetrabutylammonium perchlorate (Bu_4NClO_4) and all other chemicals were reagent grade and used as received.

Toluene solutions of gold nanoparticles (AuNPs) 10^{-2} M gold concentration containing 0.05 M tetraoctylammonium bromide (TOABr) as stabilizer were prepared according to Schiffrin.[17] On the basis of TEM analysis, the average particle size of the TOABr-stabilized gold clusters is 5 ± 1 nm. AuNPs were routinely used in 10^{-3} M gold concentration.

The compounds 6-(2,2′:5′,2″terthien-5-yl)hexane-1-thiol (T3C6SH),[18] 2,2′:5′,2″-terthiophene-5-thiol (T3SH),[8] 6-(2,2′:5′,2″-terthien-5-yl)-hexylphosphonic acid (T3C6PA),[8] and 2-bis(thien-2-yl)methylthiophene [(T)3CH][19] were prepared according to literature procedures.

^1H and ^{13}C NMR spectra were recorded on a Bruker FT 300 (300 MHz for ^1H); chemical shifts values are given in parts per million.

2-[7-Bromo-1,1-bis(thien-2-yl)heptyl]thiophene [(T)3C7Br]. BuLi (1.6 M in hexane, 7.2 mL, 11.57 mmol) was added dropwise to a stirred solution of (T)3CH (2.335 g, 8.90 mmol) and TMEDA

(14) (a) Wang, F.; Rauh, R. D.; Rose, T. L. *J. Am. Chem. Soc.* **1997**, *119*, 11106. (b) Wang, F.; Wilson, M. S.; Rauh, R. D.; Schottland, P.; Reynolds, J. R. *Macromolecules* **1999**, *32*, 4272. (c) Wang, F.; Kon, A. B.; Rauh, R. D. *Macromolecules* **2000**, *33*, 5300. (d) Wang, F.; Wilson, M. S.; Rauh, R. D.; Schottland, P.; Thompson, B. C.; Reynolds, J. R. *Macromolecules* **2000**, *33*, 2083. (e) Sebastian, R. M.; Caminade, A. M.; Majoral, J. P.; Levillain, E.; Huchet, L.; Roncali, J. *Chem. Commun.* **2000**, *6*, 507. (f) Alvarez, J.; Sun, L.; Crooks, R. M. *Chem. Mater.* **2002**, *14*, 3995. (g) Deng, S.; Locklin, J.; Patton, D.; Baba, A.; Advincula, R. C. *J. Am. Chem. Soc.* **2005**, *127*, 1744.
(15) (a) Tabakovic, I.; Kunugi, Y.; Canavesi, A.; Miller, L. L. *Acta Chem. Scand.* **1998**, *52*, 131. (b) Yamamoto, K.; Higuchi, M.; Uchida, K.; Kojima, Y. *Macromolecules* **2002**, *35*, 5782.
(16) (a) Cherioux, F.; Guyard, L.; Audebert, P. *Chem. Commun.* **1998**, *20*, 2225. (b) Cherioux, F.; Guyard, L. *Adv. Funct. Mater.* **2001**, *11*, 305. (c) Kotha, S.; Chakraborty, K.; Brahmachary, E. *Synlett* **1999**, *10*, 1621. (d) Bras, J.; Guillerez, S.; Pépin-Donat, B. *Chem. Mater.* **2000**, *12*, 2372. (e) Geng, Y.; Fechtenkötter, A.; Müllen, K. *J. Mater. Chem.* **2001**, *11*, 1634. (f) Pappenfus, T. M.; Mann, K. R. *Org. Lett.* **2002**, *4*, 3043. (g) Thomas, K. R. J.; Lin, J. T.; Tao, Y. T.; Ko, C. W. *Chem. Mater.* **2002**, *14*, 1354. (h) Ponomarenko, S. A.; Kirchmeyer, S.; Elschner, A.; Huisman, B. H.; Karbach, A.; Drechsler, D. *Adv. Funct. Mater.* **2003**, *13*, 591. (i) Pei, J.; Wang, J. L.; Cao, X. Y.; Zhou, X. H.; Zhang, W. B. *J. Am. Chem. Soc.* **2003**, *125*, 9944. (l) Nicolas, Y.; Blanchard, P.; Levillain, E.; Allain, M.; Mercier, N.; Roncali, J. *Org. Lett.* **2004**, *6*, 273.
(17) Brust, M.; Bethell, D.; Schiffrin, D. J.; Kiely, C. *Adv. Mater.* **1995**, *7*, 795.
(18) Michalitsch, R.; Lang, P.; Yassar, A.; Nauer, G.; Garnier, F. *Adv. Mater.* **1997**, *9*, 321.
(19) Sugino, M.; Ishii, A.; Hoshino, M. *Chem. Lett.* **1992**, 703.

(1.540 g, 13.25 mmol) in THF (50 mL), keeping the temperature at −78 °C. After 1 h of stirring, the reaction mixture was added dropwise to a solution of 1,6-dibromohexane (6.429 g, 26.35 mmol) in THF (25 mL), keeping the temperature at −78 °C. Stirring was kept overnight at room temperature, and then the reaction mixture was poured into water and extracted with CH_2Cl_2. The organic phase was dried (Na_2SO_4), and the solvent and excess 1,6-dibromohexane were evaporated under reduced pressure. Flash chromatography of the residue (silica gel, petrol ether) afforded the title compound (2.65 g, 70% yield) as a solid. Anal. Calcd for $C_{19}H_{21}BrS_3$: C, 53.64; H, 4.98%. Found: C, 53.52; H, 4.91%. ^{1}H NMR ($CDCl_3$): δ 1.45 (m, 6H), 1.81 (m, 2H), 2.56 (m, 2H), 3.37 (t, 2H), 6.93 (m, 6H), 7.20 (m, 3H).

2-Bromo-5-[7-bromo-1,1-bis(5-bromothien-2-yl)heptyl]thiophene [(TBr)3C7Br]. NBS (2.63 g, 14.76 mmol) was added portionwise at room temperature to a solution of (T)3C7Br (2.00 g, 4.70 mmol) in DMF (50 mL). The reaction mixture was kept under stirring overnight, poured into water, and extracted with ether. The organic phase was washed with water, dried (Na_2SO_4), and evaporated to dryness to give the title compound as an oil (2.90 g, 93% yield), which was used without any further purification for the next step. ^{1}H NMR ($CDCl_3$): δ 1.41 (m, 6H), 1.83 (m, 2H), 2.37 (m, 2H), 3.37 (t, 2H), 6.67 (d, 3H), 6.89 (d, 3H).

5-[7-Bromo-1,1-bis(2,2′-bithien-5-yl)heptyl]-2,2′-bithiophene [(T2)3C7Br]. A solution of 2-thienylmagnesium bromide (1.55 mmol) in ether (5 mL) was added dropwise in 20 min to a stirred mixture of (TBr)3C7Br (253 mg, 0.38 mmol) and $PdCl_2(PPh_3)_2$ (catalytic amount) in ether (10 mL). After being stirred under reflux for 5 h and at room temperature overnight, the reaction mixture was treated with 1 M HCl and extracted with ether. The organic phase was washed with water and dried (Na_2SO_4) and the solvent evaporated. Flash chromatography of the residue (silica gel, petrol ether/CH_2Cl_2 94:6) afforded the title compound as a low-melting solid (172 mg, 67% yield). Anal. Calcd for $C_{31}H_{27}BrS_6$: C, 55.42; H, 4.05%. Found: C, 55.31%; H, 3.99%. ^{1}H NMR ($CDCl_3$): δ 1.43 (m, 6H), 1.83 (m, 2H), 2.53 (m, 2H), 3.37 (t, 2H), 6.92 (d, 3H), 6.97 (m, 3H), 7.02 (d, 3H), 7.12 (m, 3H), 7.19 (m, 3H). HREIMS calcd, 669.962; found, 669.962.

5-Bromo-5′-[7-bromo-1,1-bis(5-bromo-2,2′-bithien-5′-yl)heptyl]-2,2′-bithiophene [(T2Br)3C7Br]. This compound was prepared following the same procedure described above for the preparation of (TBr)3C7Br, starting from (T2)3C7Br. The title compound was obtained as an oil (92% yield), which was used without any further purification for the next step. ^{1}H NMR ($CDCl_3$): δ 1.46 (m, 6H), 1.81 (m, 2H), 2.51 (m, 2H), 3.37 (t, 2H), 6.83 (d, 3H), 6.89 (d, 3H), 6.92 (d, 3H), 6.95 (d, 3H).

5-[7-Bromo-1,1-bis(2,2′:5′,2″-terthien-5-yl)heptyl]-2,2′:5′,2″-terthiophene [(T3)3C7Br]. This compound was prepared following the same procedure described above for the preparation of (T2)-3C7Br, starting from (T2Br)3C7Br. Flash chromatography of the residue (silica gel, petrol ether/CH_2Cl_2 8:2) afforded the title compound as a solid (37% yield), mp 153 °C. Anal. Calcd for $C_{43}H_{33}BrS_9$: C, 56.25; H, 3.62%. Found: C, 56.12%; H, 3.55%. ^{1}H NMR ($CDCl_3$): δ 1.45 (m, 6H), 1.83 (m, 2H), 2.56 (m, 2H), 3.39 (t, 2H), 6.93 (d, 3H), 7.02 (m, 12H), 7.15 (m. 3H), 7.21 (m, 3H). ^{13}C NMR ($CDCl_3$): δ 25.40, 27.95, 29.09, 32.68, 33.76, 44.48, 51.19, 122.66, 123.62, 124.20, 124.40, 127.12, 127.82, 135.95, 136.19, 136.47, 137.09, 150,39.

7,7,7-Tris(2,2′:5′,2″-terthien-5-yl)-heptane-1-thiol [(T3)3C7SH]. A mixture of (T3)3C7Br (225 mg, 0.24 mmol), thiourea (20 mg, 0.26 mmol), and ethyleneglycol (2 mL) was heated at 130 °C for 6 h. Tetraethylene pentamine (23 mg, 0.12 mmol) was added and the resulting mixture heated at the same temperature for 3 h and then cooled to room temperature. 1 N HCl was added and the reaction mixture extracted with CH_2Cl_2. The organic phase was washed with water and dried (Na_2SO_4) and the solvent evaporated. Flash chromatography of the residue (silica gel, petrol ether/CH_2Cl_2 75:25) afforded the title compound (136 mg, 65% yield). Anal. Calcd for $C_{43}H_{24}S_{10}$: C, 59.27; H, 3.93%. Found: C, 59.05%; H, 3.76%. ^{1}H NMR ($CDCl_3$): δ 1.35 (t, 1H), 1.39 (m, 4H), 1.59 (m, 4H), 2.53 (t, 2H), 2.57 (m, 2H), 6.97 (d, 3H), 7.03 (m, 3H), 7.05 (m, 6H), 7.07 (d, 3H), 7.19 (d, 3H), 7.23 (d, 3H). ^{13}C NMR ($CDCl_3$): δ 24.55, 25.71, 28.43, 29.52, 33.89, 44.69, 51.41, 122.75, 123.65, 124.33, 124.54, 127.24, 127.87, 136.08, 136.21, 136.71, 137.34, 150,66. FABMS, *m*/*z* 871 $(M + H)^+$.

2.2. Substrates and Film Formation. Gold electrodes were 1 × 4 cm^2 sheets which were previously treated for 1 min with hot mixed chromic acid ($K_2Cr_2O_7$ in 96% H_2SO_4) and then carefully washed with Milli-Q water and dried.

ITO/glass electrodes were 1 × 4 cm^2 indium tin oxide one-side-coated float-glass sheets (20 Ω sq^{-1} from Merck-Balzers) which were cleaned with acetone immediately before use. The ITO microstructure consists of grains ca. 100 nm in diameter and 3 nm high (average). A much thinner ITO deposit is present also on the glass side of the sheet.

For the preparation of transparent gold-coated electrodes, the ITO/glass electrodes were treated with 3-mercaptopropyl-trimethoxysilane (MTS),[20] providing a surface bearing free thiol groups and subsequently with toluene solution of AuNPs for 18 h, which deposited a monolayer of them on the thiol surface (ITO/ MTS/ AuNPs layer).

Terthiophene-thiol monolayers were prepared from 5×10^{-4} M solutions of the thiol in an EtOH/CH_2Cl_2 1:2 v/v mixture, allowing the gold substrate to react for 16 h.[21] MP4 monolayers were prepared from 5×10^{-4} M solution in EtOH with dipping times of 15 min, which was more than enough for the formation of a full (1−2 nm thick) monolayer.[22]

2.3. Apparatus and Procedure. Electrochemical experiments were performed in acetonitrile + 0.1 M Bu_4NClO_4 at 25 °C under nitrogen in three electrode cells. The counter electrode was platinum; unless otherwise stated the reference electrode was a silver/0.1 M silver perchlorate in acetonitrile (0.34 V vs SCE). The voltammetric apparatus (AMEL, Italy) included a 551 potentiostat modulated by a 568 programmable function generator and coupled to a 731 digital integrator.

Electronic spectra were obtained from a Perkin-Elmer Lambda 15 spectrometer. Unless otherwise stated the absorbance data of mono- and multilayers are given as measured, i.e., for the sum of the ITO and glass sides, since the same level of functionalization is obtained at both sides of the electrode.

Measurements of the sheet resistance of the multilayers were performed on the glass side of the substrate with the four-probe technique using a Kuliche-Soffa head (UK) with a Keithley 220 programmable current source and a Keithley 195A digital multimeter.

Atomic force microscopy (AFM) was performed in contact mode in air at room temperature using a DME DS 95-200 Dualscope STM equipped with contact mode silicon tips with nominal tip radius of 10 nm. Topography and friction force images were recorded simultaneously.

(20) Goss, C. A.; Charych, D. H.; Majda, M. *Anal. Chem.* **1991**, *63*, 85.
(21) Liedberg, B.; Yang, Z.; Engquist, I.; Wirde, M.; Gelius, U.; Gotz, G.; Bauerle, P.; Rummel, R. M.; Ziegler, C.; Gopel, W. *J. Phys. Chem. B* **1997**, *101*, 5951.
(22) (a) Delamarche, E.; Geissler, M.; Wolf, H.; Michel, B. *J. Am. Chem. Soc.* **2002**, *124*, 3834. (b) Trimbach, D. C.; Al-Hussein, M.; de Jeu, W. H.; Decre, M.; Broer, D. J.; Bastiaansen, C. W. M. *Langmuir* **2004**, *20*, 4738.

Scheme 1

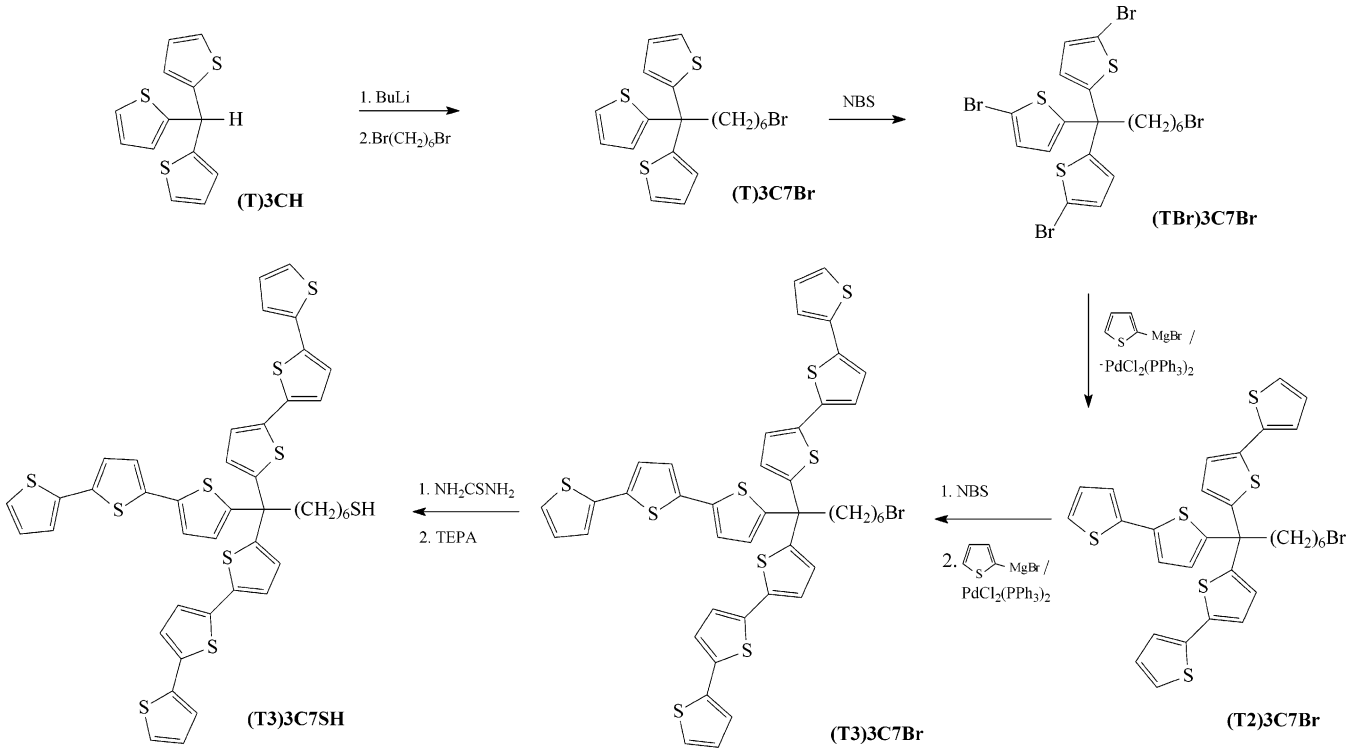

Conducting probe AFM (CP-AFM) was used for bulk resistance measurements of layers on conducting substrates. The AFM tips used were plateau-style tips (5 μm diameter) from Pacific Nanotechnology. AFM tips were coated with metal using a Balzers thermal metal evaporator at a pressure of 10^{-6} Torr. Tips were coated with 100 nm of gold at a rate of 0.1 nm s^{-1} after the deposition of a 5 nm Cr adhesion layer. Current−voltage measurements were made using the AFM instrument above. Junctions were formed by bringing gold-coated AFM tips into contact with layers on ITO or gold substrates to a force of 10 nN. A Keithley 236 source/measure unit was used to apply a voltage to the AFM tip, and the substrate was grounded through a Keithley 6517 DC ammeter. For a typical data-taking session with a single gold-coated tip, at least 5 $I-V$ traces per layer were measured to give an average resistance value.

3. Results and Discussion

3.1. Synthesis of the Compounds. As reported in the Experimental Section, compounds T3C6SH, T3SH, and T3C6PA were prepared following known procedure, while (T3)3C7SH was prepared as depicted in Scheme 1.

(T)3C7Br, prepared from (T)3CH through reaction with BuLi and alkylation with 1,6-dibromohexane, was brominated with NBS and the bromo derivative (TBr)3C7Br was reacted with 2-thienylmagnesium bromide in the presence of $PdCl_2(PPh_3)_2$ to give (T2)3C7Br. A subsequent bromination in the α thiophenic positions, followed by a cross-coupling reaction with 2-thienylmagnesium bromide, afforded (T3)3C7Br. This compound was converted to the thiol (T3)3C7SH via formation of the corresponding isothiouronium salt that was subsequently cleaved by tetraethylene pentamine.[23]

(23) Michalitsch, R.; ElKassmi, A.; Yassar, A.;Garnier, F. *J. Heterocycl. Chem.* **2001**, *38*, 649.

3.2. Monolayers. *3.2.1. Monolayering AuNPs on Thiol-Primed ITO.* For the preparation of transparent gold-functionalized electrodes, AuNPs are adsorbed on an ITO/glass electrode. The production of such monolayers on hydroxylated surfaces was previously reported in the literature[24] but no kinetic investigation was performed. In this section we report the time-resolved formation of the AuNPs monolayer, to be compared with the analogous formation on T3-primed surfaces reported in the next section.

The ITO/glass surface was first derivatized with 3-mercaptopropyl-trimethoxysilane,[20] providing a surface densely covered with free thiol groups. Immersion of the substrate in the ruby-red toluene solution of AuNPs deposits a monolayer of them on the thiol surface.

The produced monolayer gives a maximum absorption at around 550 nm (Figure 1a) with a limiting absorbance A_L of 0.05 au obtained after a dipping time of 18 h. The spectrum thus features the typical surface plasmon (SP) absorbance maximum bathochromically shifted from the solution value (525 nm) mainly due to changes in the dielectric environment since the particles are attached to ITO.

(24) (a) Westcott, S. L.; Oldenburg, S. J.; Lee, T. R.; Halas, N. J. *Langmuir* **1998**, *14*, 5396. (b) Jiang, P.; Cizeron, J.; Bertone, J. F.; Colvin, V. L. *J. Am. Chem. Soc.* **1999**, *121*, 7957. (c) Zhang, J.; Lahtinen, R. M.; Kontturi, K.; Unwin, P. R.; Schiffrin, D. J. *Chem. Commun.* **2001**, 1818. (d) Guari, Y.; Thieuleux, C.; Mehdi, A.; Reye, C.; Corriu, R. J. P. *Chem. Commun.* **2001**, 1374. (e) Fleming, M. S.; Walt, D. R. *Langmuir* **2001**, *17*, 4836. (f) Park, S.; Weaver, M. J. *J. Phys. Chem. B* **2002**, *106*, 8667. (g) Chen, C.; Tsai, C. Y.; Ko, F.; Pun, C.; Chen, H.; Chen, P. *Jpn. J. Appl. Phys. Part 1* **2004**, *43*, 3843. (h) Zhang, J.; Kambayashi, M.; Oyama, M. *Electrochem. Commun.* **2004**, *6*, 683. (i) Fu, Y.; Yua, R.; Xu, L.; Chai, Y.; Zhong, X.; Tang, D. *Biochem. Eng. J.* **2005**, *23*, 37. (l) Li, J.; Xu, C.; Zhang, Z.; Wang, Y.; Peng, H.; Lu, Z.; Chan, M. *Sens. Actuators B* **2005**, *106*, 378. (m) Tang, D.; Yuan, R.; Chai, Y.; Liu, Y.; Dai, J.; Zhong, X. *Anal. Bioanal. Chem.* **2005**, *381*, 674. (n) Sheibley, D.; Tognarelli, D. J.; Szymanik, R.; Leopold, M. C. *J. Mater. Chem.* **2005**, *15*, 491.

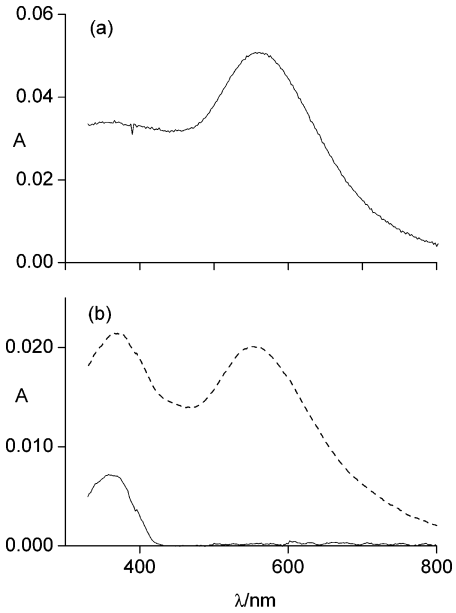

Figure 1. UV−vis spectra of (a) ITO/MTS/AuNPs monolayer and (b) (—) ITO/T3C6PA and (- - -) ITO/T3C6PA/AuNPs monolayers.

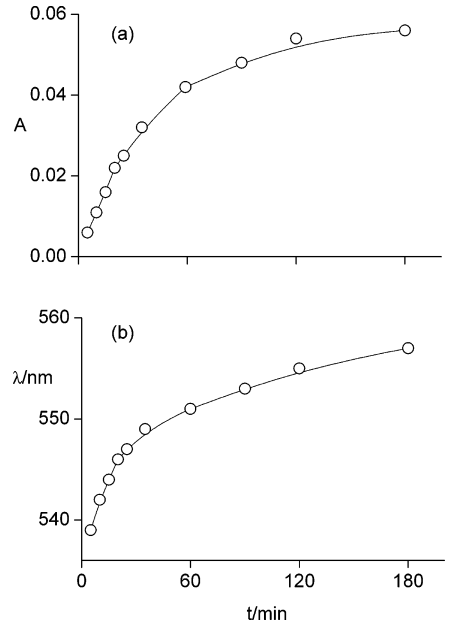

Figure 2. UV−vis kinetics of AuNPs monolayer formation on ITO/MTS: (a) absorbance and (b) maximum wavelength.

No such absorption is recorded on similarly treated bare ITO/glass.

The kinetics of gold functionalization has been followed by spectral analysis of maximum absorbance and maximum wavelength with time (Figure 2). The adsorbance A follows a law of exponential saturation:

$$A = A_L[1 - \exp(-kt)] \qquad (1)$$

with a constant $k = 0.02\ \text{min}^{-1}$, which means that saturation is practically achieved in 2−3 h of adsorption.

The maximum wavelength increases with time in a similar fashion (Figure 2b). It is noteworthy that the plot of λ_{max} vs absorbance (Figure 3) is linear. Since the absorbance is a measure of the amount of adsorbed gold particles and λ_{max} of AuNPs is in practice linearly linked to the particle

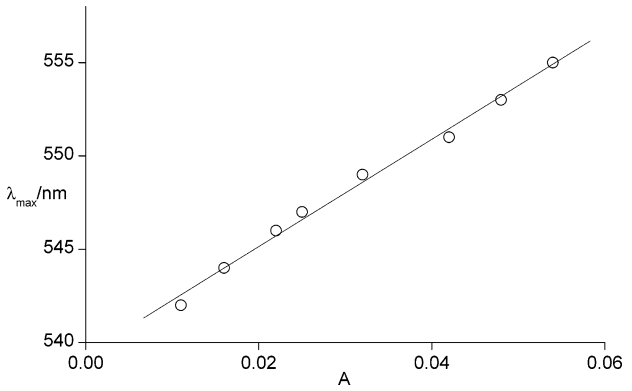

Figure 3. SP-band maximum wavelength vs absorbance in the UV−vis kinetics of AuNPs monolayer formation on ITO/MTS.

diameter,[25] it might be imagined that the red shift observed in monolayer formation is due to an increase of the size of the adsorbed particles. Yet the adsorption process occurs on the thiol sites of the surface and not on previously adsorbed particles, which are individually capped, so that another reason is required to account for the observation. In fact, when the metal nanoparticle volume (or surface) fraction is high, dipole−dipole interactions between neighboring nanoparticles are present; i.e., the oscillating dipoles of neighboring particles influence the frequency of a central particle.[26] For this reason in layers of gold nanoparticles surrounded by inert silica shells of varying thicknesses, the absorption colors range from blue for densely packed metal spheres to light red for well-separated particles.[26] Similar gold aggregates show a progressive red shift as interparticle spacers of decreased length are used.[27] Thus, the observed red shift is entirely due to increased interactions among the progressively adsorbed particles.

The maximum gold coverage of the monolayers has been evaluated by CV. In fact, gold is oxidized in oxoacids to produce a gold oxide surface of well-defined composition.[28] The CV of a gold sheet electrode in 0.1 M $HClO_4$ between 0.0 and 1.5 V vs SCE shows an oxidation peak at 1.2 V and a backward reduction peak at 0.8 V (at a scan rate of 0.1 V s^{-1}). The relevant stored surface charge is 400 uC cm^{-2}.[28]

We have found a similar stable response in the ITO/MTS/AuNPs layer. No response is given by the bare ITO after AuNPs treatment, in agreement with the spectral result given above. The response of the fully gold-coated monolayers, reproducible within 10%, gives a reversible charge of 500 μC cm^{-2}. From this figure, the charge per unit area of gold, and the mean particle size (5 nm diameter), a surface particle density of 1.6×10^{12} particles cm^{-2} was evaluated. From the SP absorbance of the layer (0.05 for a two-side coverage) and that of the toluene solution (apparent extinction coefficient 2×10^3 M^{-1} cm^{-1} as gold moles), the optically derived value is 2×10^{12} particles cm^{-2}; i.e., the electrochemical and optical values are in very good agreement.

(25) Link, S.; El-Sayed, M. A. *J. Phys. Chem. B* **1999**, *103*, 4212.
(26) Ung, T.; Marza, L. M. L.; Mulvaney, P. *J. Phys. Chem. B* **2001**, *105*, 3441.
(27) Huang, H. Y.; Chen, W. F.; Kuo, P. L. *J. Phys. Chem. B* **2005**, *109*, 24288.
(28) Angerstein, H.; Conway, B. E.; Hamelin, A.; Stoichoviciou, L. *J. Electroanal. Chem.* **1987**, *228*, 429.

3.2.2. Monolayering AuNPs on Terthiophene-Primed ITO. To check the gold aggregating ability of terthiophene monolayers, we have functionalized an ITO-glass substrate with the terthiophene phosphonic acid T3C6PA, following the previously published procedure,[8] and subsequently treated it with the gold colloidal solution. The UV−vis spectra (Figure 1b) of this ITO/ T3C6PA layer shows the weak band of the adsorbed terthiophene at 360 nm and after gold treatment the resulting ITO/T3C6PA/AuNPs monolayer displays an additional strong band at 590 nm due to the gold cluster layer. The produced gold monolayer gives a limiting absorbance of 0.02 au in some hours. This value is lower than that for the MPS layer which may be accounted for by the lower density of coordinating sites and their less favorable orientation in the terthiophene case.

The kinetics of gold functionalization shows that adsorbance follows once more a law of exponential saturation with a constant $k = 0.05$ min^{-1}, namely, 2−3 times faster than that with MTS. Also in this case the maximum wavelength increases with time. The kinetics is not so different from that of the MTS-primed layer. In any case the rate-determining step for the reaction may not be simply the adsorption of gold particles on the T3 moieties (for the T3-primed surface) or the homolytic cleavage of the S−H bond with accompanying S−Au bond formation (for the thiol-primed surface)[1b] but may involve the displacement of the AuNP-stabilizing TOABr shell, which tends to make similar the rates of the two mechanisms.

This result has opened up the possibility of layering gold nanoparticles on oligothiophene-primed surfaces and building multilayers therefrom. Such multilayering processes are described in the following sections.

3.2.3. Star Terthiophene-Thiol Monolayers. SA gold thiolate monolayers from terthiophene disulfide and terthiophene-undecyl disulfide have been previously reported.[21] T3C6SH has been previously used for monolayer formation on platinum[29] and we have later investigated thoroughly its adsorption on gold and the electrochemical behavior of the SA layers.[8]

Here we report the characterization of SAMs of the star terthiophene-thiol (T3)3C7SH on gold.

(a) Electrochemistry. The (T3)3C7SH SAM coverage on a gold electrode was first evaluated by reductive stripping. The monolayers are in fact irreversibly reduced in 0.5 M KOH in two processes at peak potentials $E_p = -1.05$ and −1.15 V vs SCE (Figure 4a) with the overall passage of 50 μC cm^{-2}. The latter value, compared with that of a full alkylthiol monolayer (100 μC cm^{-2}),[30] indicates a rather dense coverage, considered the bulky star heads. Monolayers of T3SH are irreversibly reduced (T3C6SH monolayers are not)[8] with the passage of ca. 100 μC cm^{-2},[8] which allows one to extrapolate that the coverage of the linear T3C6SH is twice that of the star compound, clearly due to steric effects.

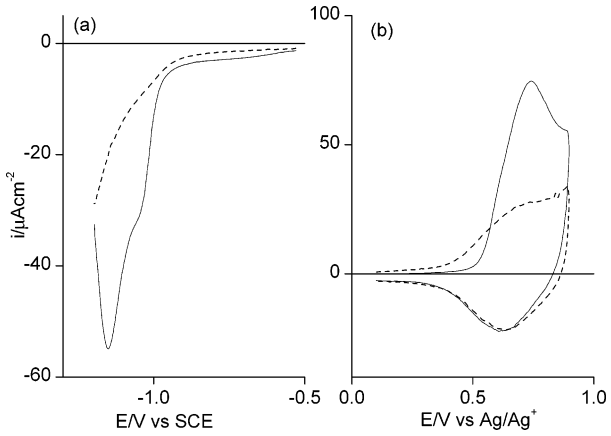

Figure 4. Cyclic voltammograms of (T3)3C7SH monolayer on gold. (a) Reduction in 0.5 M KOH and (b) oxidation in acetonitrile + 0.1 M Bu_4NClO_4. Scan rate: 0.1 V s^{-1}. (—) first and (- - -) subsequent cycles.

The oxidation of (T3)3C7SH SAMs was performed in acetonitrile + 0.1 M Bu_4NClO_4 with CV up to 0.9 V at a scan rate of 0.1 V s^{-1}. On the first cycle the monolayer is irreversibly oxidized (Figure 4b) at the same E_p value (0.73 V) of the T3C6SH monolayer. The total oxidation charge Q_{ox} involved in the CV cycle is 200 μC cm^{-2}.

After the first oxidation cycle the voltammogram displays a reversible redox process at $E^0 = 0.65$ V (Figure 4b), which is not modified in further CVs. This process, which involves ca. 75 μC cm^{-2}, corresponds to the two-electron reversible oxidation of the T6 moieties which are formed by surface coupling (Scheme 2). The charge is 1.5 times that involved in the cathodic stripping (1 F mol^{-1}), and since it corresponds to the number of efficient self-coupling events, it indicates that the cross-coupling to T6 is quite extensive, corresponding to the average involvement of 1.5 terthiophene subunits per adsorbed star molecule.

Differently from the crystalline α,ω-dimethylsexithiophene films, which display two separate redox processes at 0.5 and 0.7 V,[31] here the T6 oxidation is a single broad cycle at an intermediate potential, which reflects the absence of side interactions stabilizing the radical cation form in the crystalline samples and agrees with the formation of isolated T6 bridges on the gold surface.

In connection with the described T3 dimerization it must be reminded that some papers have been previously devoted to the postpolymerization of self-assembled monolayers of linear terthiophenes[29,32] or of dendrimers bearing linear terthiophene arms.[33]

(b) UV−Vis Spectroscopy. For a spectroscopic analysis (T3)3C7SH has been adsorbed on an ITO/MTS/AuNPs electrode (Figure 5), producing a shift of the gold SP band from 550 to 575 nm with enhanced intensity and the appearance of the terthiophene band at 375 nm. From the

(29) Michalitsch, R.; Kassim, E. I.; Yassar, A.; Lang, P.; Garnier, F. *J. Electroanal. Chem.* **1998**, *457*, 129.
(30) Kakiuchi, T.; Usui, H.; Hobara, D.; Yamamoto, M. *Langmuir* **2002**, *18*, 5231.
(31) Zotti, G.; Schiavon, G.; Berlin, A.; Pagani, G. *Chem. Mater.* **1993**, *5*, 620.
(32) (a) Berlin, A.; Zotti, G.; Schiavon, G.; Zecchin, S. *J. Am. Chem. Soc.* **1998**, *120*, 13453. (b) Michalitsch, R.; Nogues, C.; Najari, A.; Elkassmi, A.; Yassar, A.; Lang, P.; Garnier, F. *Synth. Met.* **1999**, *101*, 5.
(33) (a) Roncali, J.; Thobie-Gautier, C.; Brisset, H.; Favart, J. F.; Guy, A. *J. Electroanal. Chem.* **1995**, *381*, 257. (b) John, H.; Bauer, R.; Espindola, P.; Sonar, P.; Heinze, J.; Mullen, K. *Angew. Chem., Int. Ed.* **2005**, *44*, 2447.

Scheme 2

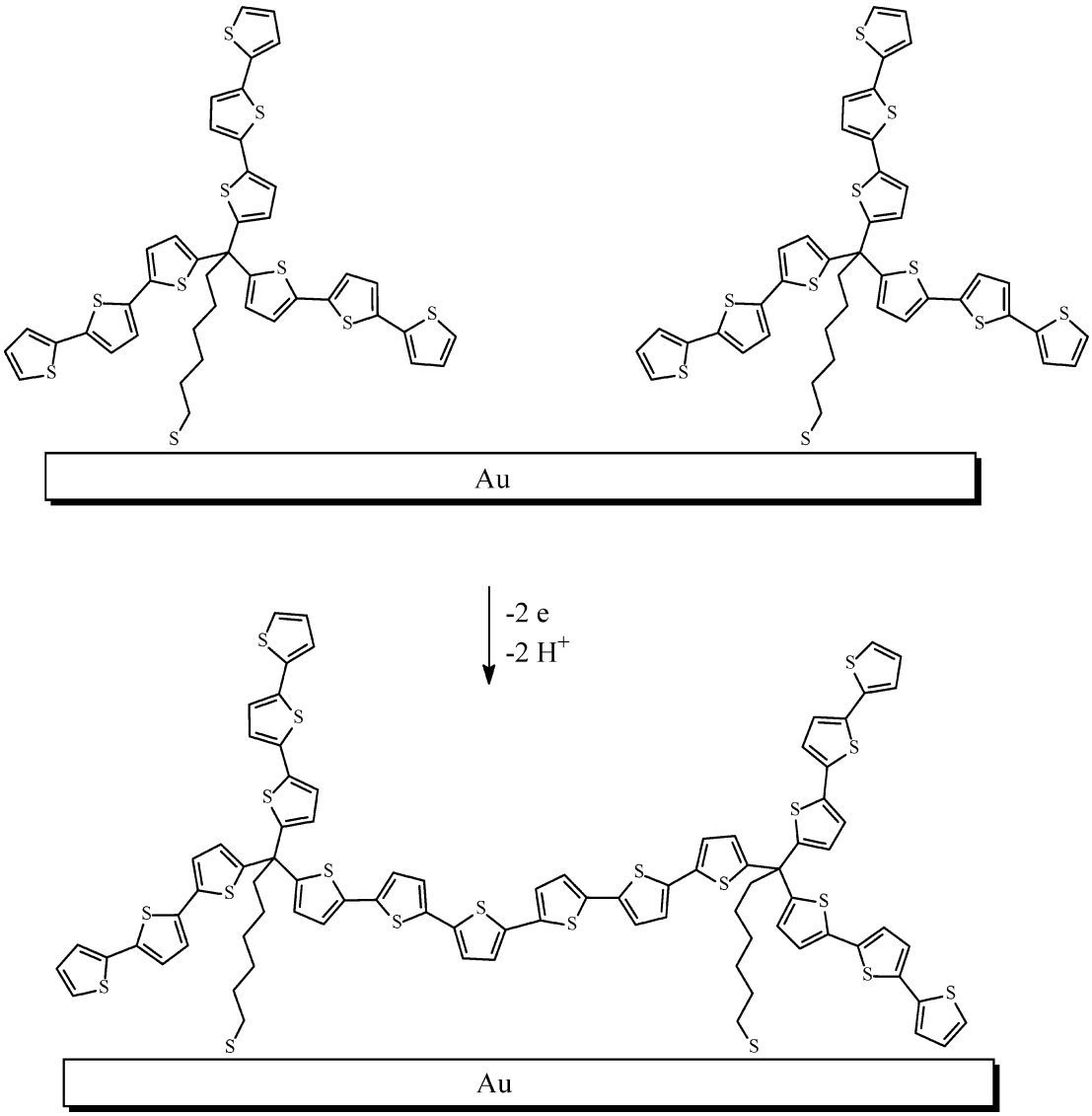

absorbance of the latter (0.030), the extinction coefficient of terthiophene (2.5×10^4 M^{-1} cm^{-1})[34] and considering that both sides of the ITO-glass are functionalized and that the star molecule bears three terthiophene arms, the degree of coverage of the gold-coated ITO electrode is 2×10^{-10} mol cm^{-2}.

For comparison, T3C6SH adsorbed on ITO/MTS/AuNPs produces a similar shift of the gold SP band with enhanced intensity and the appearance of the terthiophene band at 370 nm. The latter displays the same absorbance of (T3)3C7SH so that the degree of coverage is in this case 6×10^{-10} mol cm^{-2}. It is therefore confirmed that the surface density of the linear terthiophene molecules is 2−3 times that of the star terthiophene compound.

The changes of the characteristics of the SP band upon SA may be in principle attributed to changes in the dielectric surrounding the particles[35] but this interpretation has been ruled out by the results with another thiol, namely, hexadecylthiol. Differently from the terthiophene-based thiols, hexadecylthiol adsorbed on ITO/MTS/AuNPs does not produce appreciable changes in the SP band. Thus, it is argued that the terthiophene moieties either cause a partial aggregation of the gold clusters or more likely interact with their surfaces by lateral adsorption. In this connection we have found that treatment of ITO/MTS/AuNPs with a terthiophene solution in toluene causes the same changes of the SP absorption.

The self-coupling oxidation of (T3)3C7SH gives the expected spectral changes (Figure 5) from the band at 375 nm of terthiophene to that of T6 at 450 nm, appearing as a differential increase (Figure 5b) since only one side of the ITO glass is electrochemically modified.

3.3. Multilayers. *3.3.1. MP4/AuNPs Multilayers.* We have first checked the formation of gold multilayers with a polythiol spacer for a significant comparison with the multilayers from the oligothiophene-thiols here investigated, in particular, with the star-shaped one.

(34) Chosrovian, H.; Rentsch, S.; Grebner, D.; Dahm, D. U.; Birckner, E.; Naarmann, H. *Synth. Met.* **1993**, *60*, 23.
(35) Doron-Mor, I.; Cohen, H.; Barkay, Z.; Shanzer, A.; Vaskevich, A.; Rubinstein, I. *Chem. Eur. J.* **2005**, *11*, 5555.

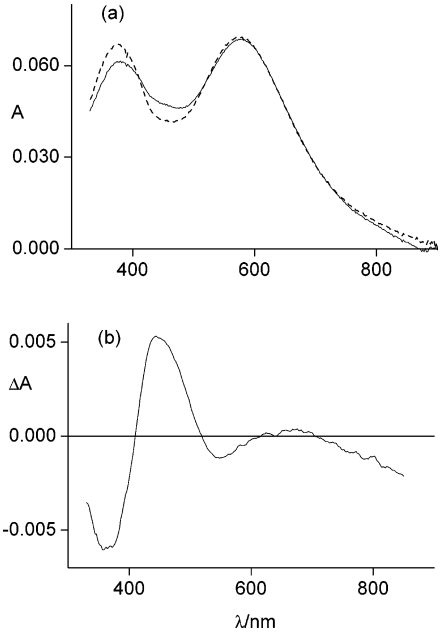

Figure 5. (a) UV−vis spectrum of (T3)3C7SH monolayer on ITO/MTS/AuNPs (- - -) before and (—) after oxidative coupling; (b) differential spectrum.

Formation of gold colloid multilayers is a documented procedure.[36−38] With use of dithiols as the spacer units, thin layer-by-layer films attached to a solid substrate have been prepared.[36−38] Such materials show conductivities that mimic the behavior of semiconductors and that depend markedly on the length of the dithiol used to link the gold particles together.

We selected MP4 as a commercially available star-shaped polythiol which was previously used for positive microcontact printing on gold.[22] The solution-formed SAM acquires the most dense packing of a conformation that, besides the thiol groups that have reacted with the gold, also has thiol entities that stick out to the interface.[22] A full monolayer 1.9 nm thick is obtained.[22b]

When the MP4-coated ITO/MTS/AuNPs electrode is immersed in colloidal gold solution, additional AuNPs binding takes place. Repetitive dips into the organic cross-linker and colloidal gold solution (15 min for the cross-linker, 120 min for the colloid, with copious rinsing between immersions) leads to the formation of gold colloid multilayers.

As shown in Figure 6, the gold coverage, given by the intensity of the SP band, increases linearly with the number of dipping cycles at a rate of 0.10 au bilayer^{-1} (Figure 6b). From this value we evaluate a step increase of surface particle density of ca. 4×10^{12} particles cm^{-2} bilayer^{-1}. A progressive shift of the SP maximum (Figure 6b) is once more observed.

Surface particle densities per bilayer for the investigated multilayers are summarized in Table 1.

3.3.2. T3C6SH/AuNPs and (T3)3C7SH/AuNPs Multilayers. T3C6SH adsorbed on ITO/MTS/AuNPs has been exposed to AuNPs and then with T3C6SH solutions alternating every 2 h. The amounts of both gold and T3C6SH increase linearly with the number of dipping cycles and in particular the SP gold absorbance increases at a rate of 0.04 au bilayer^{-1}.

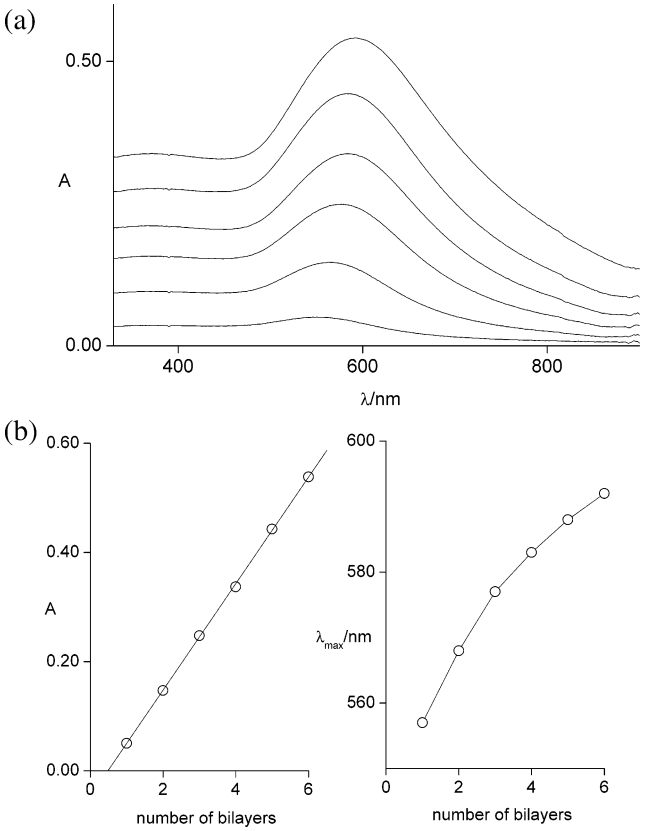

Figure 6. (a) UV−vis spectra of subsequent AuNPs/MP4 bilayers on ITO/MTS; (b) SP absorbance and maximum wavelength vs number of bilayers.

Table 1. Surface Density per Bilayer of Gold Particles N_p and Surface Resistivity R for (Thiol/AuNPs)$_5$ Multilayers

thiol	N_p (particles cm^{-2} bilayer^{-1})	R (Ω sq^{-1})
MP4	4×10^{12}	9×10^{6}
T3C6SH	1.5×10^{12}	1×10^{7}
(T3)3C7SH	1.5×10^{12}	2×10^{7}
(T3)3C7SH(Ox)	5.5×10^{12}	4×10^{7}

(T3)3C7SH adsorbed similarly on ITO/MTS/AuNPs produces the same trend with the same increase rate (Figure 7). This corresponds to the same coverage in terms of terthiophene moieties and indicates that the shape of the T3-scaffold has no influence on the gold adsorption.

Gold clusters constituting the layers mutually interact to a noticeable extent. This is evidenced by the progressive shift of the SP maximum absorption from 550 to 610 nm (Figure 7b), which is even more pronounced than that observed with MP4 (see above). It is clear that this result arises from the mediation of the oligothiophene moieties which originates a stronger interaction among AuNPs.

3.3.3. (T3)3C7SH(Ox)/AuNPs Multilayers. We have also investigated the formation of multilayers of AuNPs with T6-coupled (T3)3C7SH, which will be hereafter named (T3)-3C7SH(Ox). To this end (T3)3C7SH adsorbed on gold or on ITO/MTS/AuNPs has been alternated with AuNPs after being oxidatively coupled to (T3)3C7SH(Ox).

We have followed the multilayer formation monitoring both the oligothiophene and the gold step-by-step growth.

(36) Brust, M.; Bethell, D.; Kiely, C. J.; Schiffrin, D. J. *Langmuir* **1998**, *14*, 5425.
(37) Musick, M. D.; Keating, C. D.; Keefe, M. H.; Natan, M. J. *Chem. Mater.* **1997**, *9*, 1499.
(38) Supriya, L.; Claus, R. O. *Chem. Mater.* **2005**, *17*, 4325.

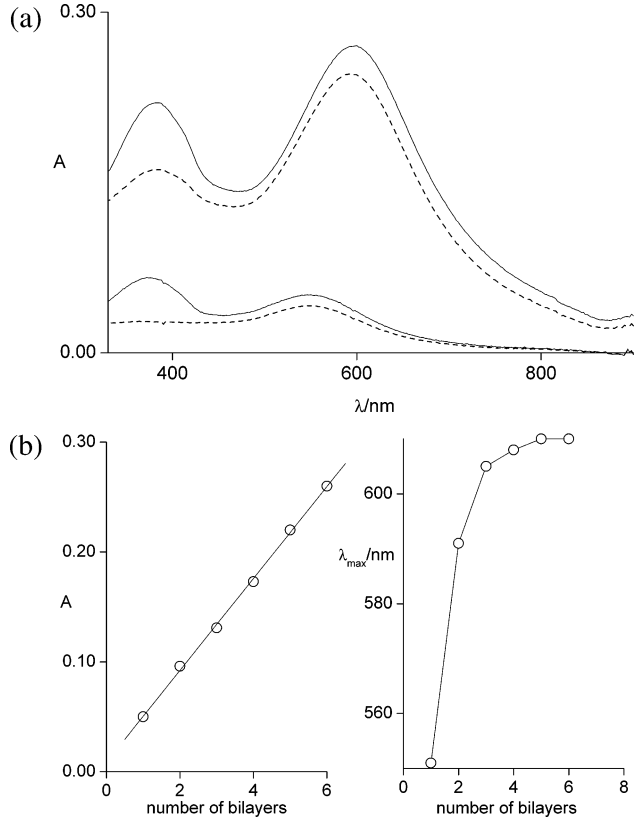

Figure 7. (a) UV−vis spectra of alternating (- - -) AuNPs and (—) (T3)-3C7SH monolayers (first and sixth bilayers only, for clarity) on ITO/MTS; (b) SP absorbance and maximum wavelength vs number of bilayers.

The redox charge has shown that (T3)3C7SH(Ox) on gold increases linearly with the number of dipping cycles at a rate of 70 μC cm^{-2} bilayer^{-1}. On the ITO/MTS/AuNPs electrode, where (T3)3C7SH(Ox) increases at a comparable rate (50 μC cm^{-2} bilayer^{-1}), the SP gold absorbance of the ITO side (where oxidation occurs) increases at a rate of 0.07 au bilayer^{-1}. Thus, the step increase of gold nanoparticles is even higher than that with MP4 and 3 times higher compared with that of the T3 scaffolds. This indicates that the T6 moieties, acting through a more extended conjugative length, are more efficient in coordinating the gold particles.

3.3.4. AFM of Multilayers. The morphology of the multilayer films on ITO/MTS/AuNPs was investigated on the float glass side by dynamic mode AFM.

As a typical example, a 1 × 1 μm^2 AFM image of a (MP4/AuNPs)$_5$ multilayer shows that the film morphology is a uniform distribution of aggregates 20−50 nm wide. rms roughness analysis gives a value of ca. 4 nm. Cross sections after removal of a square window from the film using the AFM tip show a uniform thickness of 23 nm.

For the various (terthiophene/AuNPs)$_5$ multilayers similar morphologies are found and cross sections of AFM cuts show uniform thicknesses of ca. 20 nm, namely, 4 nm bilayer^{-1}.

The bilayer thickness and surface roughness of 4 nm indicate a good packing of the 5 nm gold nanoparticles in the multilayers.

All the produced multilayers are strongly bound to the substrate since they stand the scotch tape strip test with no significant loss of material.

3.3.5. Four-Probe Conductivity of Multilayers. The (MP4/AuNPs)$_5$ multilayer, taken as the reference system, displays a four-probe surface resistivity of ca. 9 × 10^6 Ω sq^{-1}. From this value and the measured thickness we can evaluate a bulk conductivity of 0.05 S cm^{-1}.

Surface resistivities for all the investigated multilayers, conjugated or not, summarized in Table 1, are in the narrow range of (1−4) × 10^7 Ω sq^{-1}. This suggests that electrons move between gold particles through the organic linkers via direct nonresonant tunneling.[39]

The conductivity does not change after 1 h of heating at 120 °C which indicates a noticeable stability of the produced gold aggregates. This supports the idea that adsorbed gold particles have little or no surface mobility and that ordered 3D solids cannot be generated this way.

Differently from this case, a decrease in the resistance of colloidal gold multilayer films, where the linker molecules were 1,6-hexanedithiol and 1,10-decanedithiol,[38] was observed upon heating, due to coalescence of the gold particles to form more conducting pathways. Therefore, it appears that the star-shaped and the T3-based linkers freeze the gold particles much more efficiently than linear nonconjugated linkers do.

3.3.6. CP-AFM of ((T3)3C7SH(Ox)/AuNPs)$_5$ Multilayers. CP-AFM analysis has been performed on (T3)3C7SH(Ox)/AuNPs multilayers to determine the conductive properties of nanometer-size films of this type, which are produced on conductive substrates only. The (MP4/AuNPs)$_5$ multilayer has been chosen as a reference system since its four-probe bulk conductivity (0.05 S cm^{-1}) could be previously measured.

The current−potential response of (MP4/AuNPs)$_5$ multilayer, resulting from applying a potential bias between the tip and the substrate, is linear (purely ohmic). The response reflects the electronic conductivity of the nanoparticle films, which occurs by electron hopping between AuNPs cores, i.e., via tunneling reactions through the intervening monolayer structures, in agreement with what has recently been reported.[40]

Also the current−potential response of ((T3)3C7SH(Ox)/AuNPs)$_5$ multilayer on ITO is linear (purely ohmic) with a resistance only fourfold that of the reference (MP4/AuNPs)$_5$ multilayer (see Table 1).

Conclusions

A new terthiophene-armed star-shaped molecule forms self-assembled monolayers on gold and the layer is oxidatively coupled with high efficiency via the terthiophene heads to sexithiophene surface bridges. Surface plasmon spectroscopy has shown that these oligothiophene-based monolayers are able to coordinate gold nanoparticles as efficiently as thiol-primed surfaces do.

Multilayering of oligothiophene-thiol and gold nanoparticles has been performed successfully. Compared with analogous structures from a linear terthiophene-thiol and a

(39) (a) Kelley, T. W.; Granstrom, E. L.; Frisbie, C. D. *Adv. Mater.* **1999**, *11*, 261. (b) Wold, D. J.; Frisbie, C. D. *J. Am. Chem. Soc.* **2000**, *122*, 2970.

(40) Zamborini, F. P.; Leopold, M. C.; Hicks, J. F.; Kulesza, P. J.; Malik, M. A.; Murray, R. W. *J. Am. Chem. Soc.* **2002**, *124*, 8958.

generic star-shaped tetrathiol, the structures display comparable mechanical strength and electrical conductivity.

This paper has shown that gold nanoparticles coordinate to oligothiophene layers producing structures similar to those traditionally formed on thiol-modified surfaces.

The main result of this investigation, namely, the first clear evidence of gold nanoparticle coordination to oligothiophenes, has opened the way to the direct functionalization of gold nanoparticles with conjugated oligomers, which is the topic of forthcoming papers.

Acknowledgment. The authors thank Mr. S. Sitran of the CNR for his technical assistance.

CM062362X